Indonesian Journal of Chemical Research

http://ojs3.unpatti.ac.id/index.php/ijcr Indo. J. Chem. Res., 11(2), 135-141, 2023

Synthesis, Evaluation, and Molecular Docking Study of 4-Monoacyl Resorcinol Against Tyrosinase Enzyme

Ade Danova[1*], Yusuf Eka Maulana[1], Elvira Hermawati[1], Warinthorn Chavasiri[2]

[1]Organic Chemistry Division, Department of Chemistry, Faculty of Mathematics and Natural Sciences, Institut Teknologi Bandung, Jalan Ganesa No.10, Bandung, West Java, 40132, Indonesia

[2]Center of Excellence in Natural Products, Department of Chemistry, Faculty of Science, Chulalongkorn University, Bangkok 10330, Thailand

[*]*Corresponding Author: adedanova@itb.ac.id*

Received: May 2023
Received in revised: July 2023
Accepted: August 2023
Available online: September 2023

Abstract

Tyrosinase is a crucial enzyme in melanin production to protect the skin from ultraviolet, leading to skin cancers. This study synthesized eight compounds of acyl resorcinol with long-chain carbon (**1**-**8**) and structurally elucidated by ^{1}H and ^{13}C NMR. The in vitro evaluation of eight synthesized compounds against tyrosinase enzyme showed that 4-heptanoyl resorcinol (**6**) exhibited high inhibitory activity compared with the kojic acid as standard. In addition, the molecular docking study demonstrated that **6** showed lower binding energy (-7.3 kcal/mol) than kojic acid (-6.9 kcal/mol) and possessed interaction with crucial residues in the active site.

Keywords:Ttyrosinase, inhibitor, molecular docking, acyl resorcinol, ^{1}H, ^{13}C NMR

INTRODUCTION

Tyrosinase (EC 1.14.18.1), a metalloenzyme containing copper ion (Cu^{2+}), is a crucial enzyme in regulating melanin production in melanocyte cells (Hassan, Ashraf, Abbas, Raza, & Seo, 2018; Pillaiyar et al., 2017; Silavi, Divsalar, & Saboury, 2012). In melanin production, tyrosinase catalyzes two different rate-limiting reactions, namely the o-hydroxylation of 4-hydroxyphenylalanine (L-tyrosine) to 3,4-dihydroxyphenylalanine (L-DOPA) (monophenolase activity) and then the oxidation of L-DOPA to dopaquinone (diphenolase activity) which will polymerize to form melanin (Ashooriha et al., 2019).

Melanin is found in many living cells like animals, plants, fungi, and bacteria, which is responsible for generating natural pigments in melanocytes through the melanogenesis process (Ashooriha et al., 2019; Pillaiyar, Manickam, & Jung, 2015; Silavi et al., 2012). In mammals, melanin is produced in the eyes, skin, hair, and brain, controlled by intrinsic factors like mutation, hormones, and the immune system, and extrinsic factors like UV radiation and chemicals (Lee, Baek, & Nam, 2016). However, uncontrol melanin production leads to high melanin content in the skin, which causes dermatological disorders (freckles, vitiligo, melasma, cancer) and non-dermatological disorders (Parkinson's disease) (Bose, Petsko, & Eliezer, 2018; Deri et al., 2016; Faig et al., 2017). People who have darker skin are more vulnerable to these diseases (Chen et al., 2015). Melanogenesis is performed by enzymatic processes like tyrosinase (Mahdavi et al., 2018). Therefore, tyrosinase has been a targeted protein in evaluating drug candidates, applicable in pharmaceutical and cosmetics.

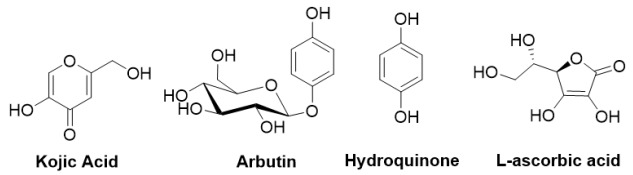

Figure 1. Several tyrosinase inhibitors

Many tyrosinase inhibitors have been reported and widely used in medicine, agriculture, and cosmetics, including kojic acid, arbutin, hydroquinone, and L-ascorbic acid in Figure 1 (Choi et al., 2010; Mann et al., 2018). Kojic acid is an available tyrosinase inhibitor in the market. However, kojic acid still has several drawbacks in cosmetics which may cause irritations in the skin due to cytotoxicity, low stability, and lipophilicity. Therefore, the development of a new tyrosinase inhibitor is still crucial to have hydrophilic and lipophilic properties to enhance dermal penetration without side effects (Karakaya, Türe, Ercan, Öncül, & Aytemir, 2019). Phenolic compounds showed high

potency as tyrosinase inhibitors because the structure is similar to kojic acid, which can be a chelating agent (Noh et al., 2009). In a previous study, 3,5-dihydroxyphenyl decanoate inhibited a mushroom tyrosinase with an IC_{50} value of 96.5 µM (Qiu, Chen, Wang, Huang, & Song, 2005).

Thus, our study aimed to make a hybrid between resorcinol as a hydrophilic moiety and acyl with long-chain carbon as a lipophilic moiety to form monoacyl resorcinol via Friedel-Craft acylation and evaluate their inhibitory activity against tyrosinase enzyme. Molecular docking was performed to investigate the interaction between monoacyl resorcinol and enzyme.

METHODOLOGY

Materials and Instrumentals

Chemicals were purchased from TCI, Sigma Aldrich, and Merck. Silica gel for column chromatography (CC) (0.063-0.200 mm) was a product of Merck Company. Tyrosinase from mushroom (EC 1.14.18.1) and L-tyrosine and kojic acid (positive control) were purchased from Sigma Aldrich. Tyrosinase inhibition was measured using the ALLSHENG AMR-100 microplate reader. TLC was performed on Merck TLC plates (0.23 mm thickness), with compounds visualized by UV light and vanillin sulfate in ethanol and then heated on a hot plate. The NMR spectra were determined using Bruker Avance 400 MHz. The hardware in this research uses a set of computers with processor chips AMD RyzenTM 9 5950x 16 core and two threads of processor @3.4 GHz, RAM 12 GB, operating system, Ubuntu 20.04.5 LTS 64-bit, and graphics processing unit (GPU) NVidia GeForce GT 610. The software in this research uses ChemOffice Professional 15.0 (Cambridge, PerkinElmer), Notepad++ (GNU General Public License), AutoDock Tools 1.5.6 (The Scripps Research Institute, USA), Autodock Vina (The Scripps Research Institute) (Trott dan Olson, 2010), BIOVIA Discovery Studio Visualizer (Dassault Systèmes), PyMol Version 2.0 (Schrodinger LLC).

General Procedure for The Synthesis of Acyl Resorcinol

Resorcinol (1.1 g, 10 mmol) was combined with anhydrous $ZnCl_2$ (3.1 g, 23.41 mmol) in long-chain carboxylic acid (5 mL) and heated at 95–100 ºC for 24 h. After completion of the reaction, the mixture was cooled to room temperature and added to ice-cold 6 N HCl (10 mL). The mixture was washed with water (20 mL), extracted with ethyl acetate, and evaporated to yield the crude product, followed by purification using column chromatography (hexane:ethylacetate= 4:1) on silica gel to afford the desired products (Liu et al., 2014).

1-(2,4-dihydroxyphenyl) butan - 1 – one (**1**). Powder, pale orange, yield: 90.0%. ^{1}H NMR (400 MHz, $CDCl_3$) δ 1.00 (*t*, 7.6 Hz, 3H), 1.75 (*sext*, 7.2 Hz, 2H), 2.86 (*t*, 7.2 Hz, 2H), 6.39 (*dd*, 2.0 Hz, 8.0 Hz, 2H), 7.65 (*d*, 8.4 Hz, 1H),12.93 (*s*, OH). ^{13}C NMR (100 MHz, $CDCl_3$) δ 205.6, 165.2, 163.2, 132.6, 113.8, 108.1, 103.6, 40.0, 18.6, 13.9.

1,1'-(4,6-dihydroxy-1,3-phenylene)bis (butan-1-one) (**2**). Powder, pale brown, yield: (2.1%). ^{1}H NMR (400 MHz, $CDCl_3$) δ 1.04 (*t*, 6H), 1.81 (*m*, 4H), 2.93 (*t*, 4H), 6.41 (*s*, 1H), 8.26 (*s*, 1H), 13.04 (*s*, OH). ^{13}C NMR (101 MHz, $CDCl_3$) δ 204.87, 168.98, 134.81, 113.31, 105.21, 39.69, 18.14, 13.96.

1-(2,4-dihydroxyphenyl)pentan-1-one (**3**). Oil, orange, yield: 56.5%. ^{1}H NMR (400 MHz, $CDCl_3$) δ 0.94 (*t*, 6.8 Hz, 3H), 1.41 (*sext*, 7.6 Hz, 2H), 1.70 (*m*, 2H), 2.88 (*t*, 7.2 Hz, 2H), 6.39 (*dd*, 2.4 Hz, 9.2 Hz, 2H), 7.64 (*d*, 9.2 Hz, 1H), 12.92 (*s*, OH). ^{13}C NMR (100 MHz, $CDCl_3$) δ 205.7, 165.3, 163.2, 132.6, 113.8, 108.1, 103.7, 37.9, 27.3, 22.6, 13.9.

1-(2,4-dihydroxyphenyl)-3-methylbutan-1-one (**4**). Oil, orange, yield: 67.4%. ^{1}H NMR (400 MHz, $CDCl_3$) δ 0.99 (*d*, 6.4 Hz, 6H), 2.24 (*m*, 1H), 2.74 (*d*, 6.8 Hz, 2H), 6.39 (*dd*, 2.4 Hz, 9.6 Hz, 2H), 7.64 (*d*, 9.2 Hz, 2H), 13.01 (*s*, OH). ^{13}C NMR (100 MHz, $CDCl_3$) δ 205.5, 165.4, 163.2, 132.8, 114.2, 108.1, 103.7, 46.9, 26.3, 22.9.

1-(2,4-dihydroxyphenyl)hexan-1-one (**5**). Oil, orange, yield: 90.6%. ^{1}H NMR (400 MHz, $CDCl_3$) δ 0.90 (*t*, 6.0 Hz, 3H), 1.35 (*m*, 3H), 1.69 (*m*, 3H), 2.87 (*t*, 7.6 Hz, 2H), 6.39 (*dd*, 2.4 Hz, 9.2 Hz, 2H), 7.64 (*dd*, 9.6 Hz, 1H), 12.93 (*s*, OH). ^{13}C NMR (100 MHz, $CDCl_3$) δ 205.8, 165.25, 163.1, 132.6, 113.8, 108.1, 103.7, 38.1, 34.1, 31.7, 31.3, 24.9, 24.5, 22.6, 22.4, 14.0.

1-(2,4-dihydroxyphenyl)heptan-1-one (**6**). Oil, orange, yield: 98.7%. ^{1}H NMR (400 MHz, $CDCl_3$) δ 0.88 (*m*, 3H), 1.31 (*m*, 6H), 1.72 (*m*, 2H), 2.88 (*t*, 7.6 Hz, 2H), 6.40 (*dd*, 2.8 Hz, 8.8 Hz), 7.65 (*d*, 9.6 Hz, 1H), 12.91 (*s*, OH). ^{13}C NMR (100 MHz, $CDCl_3$) δ 205.7, 165.3, 163.0, 132.6, 113.8, 108.1, 103.7, 38.2, 31.7, 29.2, 25.2, 22.6, 14.1.

1-(2,4-dihydroxyphenyl)octan-1-one (**7**). Oil, orange, yield: 90.0%. ^{1}H NMR (400 MHz, $CDCl_3$) δ 0.87 (*t*, 6.8 Hz, 8H), 1.67 (*m*, 5H), 2.87 (*t*, 7.6 Hz, 2H), 6.39 (*dd*, 2.8 Hz, 7.6 Hz, 2H), 7.64 (*d*, 9.6 Hz, 1H), 12.90 (*s*, OH). ^{13}C NMR (100 MHz, $CDCl_3$) δ 205.6, 165.3, 163.1, 132.5, 113.79, 108.0, 103.7, 38.2, 34.1, 29.5, 25.2, 24.8, 22.7, 14.2.

1-(2,4-dihydroxyphenyl)nonan-1-one (**8**). Oil, orange, yield: 92.0%. ^{1}H NMR (400 MHz, $CDCl_3$) δ 0.88 (*s*, 4H), 1.28 (*s*, 9H), 1.68 (*m*, 2H), 2.36 (*s*, 1H), 2.89 (*s*, 1H), 6.39 (*s*, 2H), 7.65 (*s*, 1H), 12.95 (*s*, OH). ^{13}C NMR (100 MHz, $CDCl_3$) δ 205.3, 164.9, 162.6, 132.2, 113.5, 107.7, 103.4, 37.8, 33.8, 31.6, 29.2, 24.8, 24.5, 22.4, 13.8.

Tyrosinase inhibition assay

The tyrosinase inhibitory activity was performed using 96 well microplates with modification (Larik et al., 2017). Compounds were prepared in 10% DMSO in buffer, and two-fold dilution was done to obtain various concentrations. 50 µL of the sample solution in buffer was placed in 96 well plates, then 50 µL tyrosinase enzyme from the mushroom (250 U/mL) was added, and the mixtures were incubated for 5 minutes. 50 µL of 5 mM L-tyrosine was added later as a substrate. The mixtures were then incubated further for 30 minutes. The reaction was measured at 492 nm. Kojic acid was used as a positive control. The concentration of compounds was 200 µM. The percentage of tyrosinase inhibition was calculated from the following formula (Equation 1), and IC_{50} was determined for each sample.

$$\%\ \text{Tyrosinase inhibition} = \frac{\Delta\text{Acontrol} - \Delta\text{A sample}}{\Delta\text{A control}}\ x\ 100 \quad (1)$$

ΔA control is the absorbance value at 492 nm without the test sample, and ΔA sample is the absorbance value with the mixture containing the sample.

Molecular Docking Study

The selected compounds were docked to the crystal structure of the Mushroom Tyrosinase (PDB ID: 2y9x), which was obtained from the Protein Data Bank (PDB) according to previous works (Abbasi et al., 2022; H. Berman, Henrick, & Nakamura, 2003; H. M. Berman et al., 2000; Chortani, Nimbarte, Horchani, Jannet, & Romdhane, 2019; Ismaya et al., 2011). The autodocktools 1.5.6 was prepared the crystal structure for docking the co-crystallized ligands, removing crystallographic water molecules, and adding the polar hydrogen atoms. The ChemOffice Professional 15.0 software was used to build 3D structures optimized using the MMF94 force field. The Autodock vina was used for docking simulation, where the center of the binding was defined in the protein crystal structure as hydroxyl oxygen of the co-crystallized tropolone molecule (x = -9.877, y = -26.859, z = -42.174) for the active site.

RESULTS AND DISCUSSION

Synthesis of eight acyl resorcinols (**1**-**8**) was carried out, as shown in Scheme 1. According to the previous work, resorcinol was reacted with several aliphatic acids through Friedel-Craft acylation catalyzed by zinc chloride in reflux condition for 24 hours (Liu et al., 2014).

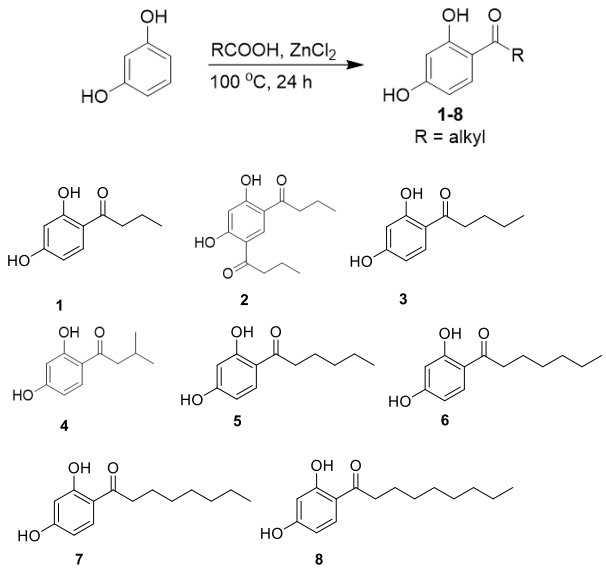

Scheme 1. Products of Friedel-Craft acylation

However, the 4,6-diacylation product (**2**) was also formed in the reaction between resorcinol and butyric acid due to excess butyric acid, but the other reaction was not formed. It might be different reactivity and steric hindrance from long-chain carbon.

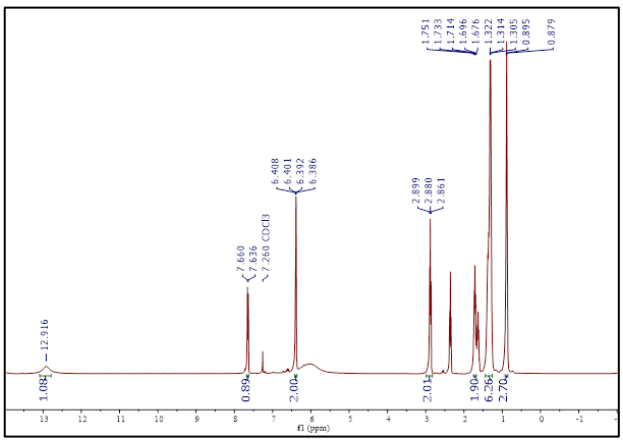

Figures 2. ^{1}H NMR spectra of compound **6** in $CDCl_3$

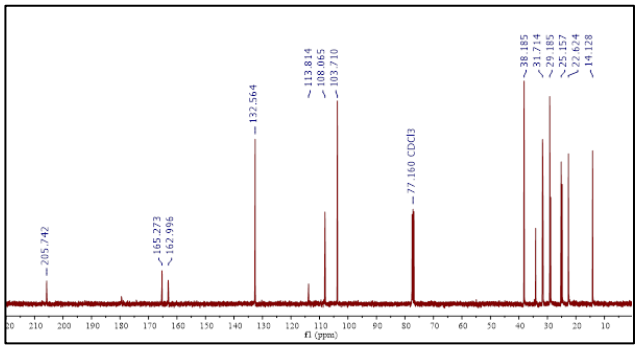

Figures 3. ^{13}C NMR spectra of compound **6** in $CDCl_3$

This study determined the products using ^{1}H and ^{13}C NMR spectroscopy. As representatives to explain the structural elucidation, **6** was selected. In ^{1}H NMR spectra, **6** showed a singlet proton at δ_H 12.91 belonged to OH closed to the carbonyl group to form hydrogen bonding. The ABX type shown in the spectra at δ_H 6.39 (*dd*, 2.8 Hz, 8.8 Hz, 2xCsp^2-H) and 7.65 (*d*, 9.6 Hz, 1xCsp^2-H) indicated that the three protons were on *ortho*, *meta*, and *para* positions. Proton signals at δ_H 0.89 (*m*, 3H), 1.31 (*m*, 6H), 1.72 (*m*, 2H), and 2.88 (*t*, 7.6 Hz, 2H) belonged to long-chain carbons. In addition, the ^{13}C NMR spectra showed a carbonyl signal at δ_C 205.7. Moreover, signals of six carbons sp^2 were shown at δ_C 165.3, 163.0, 132.6, 113.8, 108.1, 103.7 belonged to the phenyl ring, and six carbons sp^3 at δ_C 38.2, 31.7, 29.2, 25.2, 22.6, 14.1 belonged to long-chain carbons.

Table 1. *In vitro* tyrosinase inhibition of acyl resorcinols (1-8)

No	% Inhibition (200 μM)[a]	±SD
1	37.655	1.033
2	6.144	2.152
3	40.586	2.561
4	20.857	1.015
5	45.434	1.863
6	79.256[b]	1.953
7	33.033	1.757
8	22.379	3.109

[a]The experiment was conducted in triplicate. [b]Inhibition of **6** (20 μM) = 49.380±2.303%. [c]IC_{50} of Kojic Acid = 36.08±1.075 μM.

Eight synthesized compounds were evaluated in vitro inhibitory activity against tyrosinase from mushrooms as previous method (Larik et al., 2017). As shown in Table 1, 4-monoacyl resorcinol with carbon sp^3 (R= alkyl) from three to six carbons (1, 3, 5, 6) showed an increase in inhibitory activity from 37.6, 40.6, 45.4, and 79.3%, respectively. However, 4-monoacyl resorcinol **7** and **8** with seven and eight carbon sp^3 declined more than 50% inhibitory activity against tyrosinase, that hydrophile-lipophile balance properties could cause. Moreover, 4-isovaleryl resorcinol (**4**) decreased a half of **3** inhibitory activity, and 4,6-dibutanoyl resorcinol (**2**) also dropped more than 6-fold inhibitory activity compared with **1** due to steric hindrance. This result suggests that **6** with six carbon sp^3 (R= alkyl) is the best inhibitor in this series.

Table 2. PDB code, native ligand, and validation result of redocking

PDB Code	Superimposed Native & redocking	Binding energy (kcal/mol)	Interactions over tyrosinase	RMSD (Å)	Binding similarity(%)
2y9x	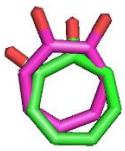 Tropolone	-5.6	**van der Waals:** His259, Asn260, Met280, Gly281, Phe264, Ala286, Phe292, Cu401 **H-bond:** His61, His263, Ser282 ***π-σ*:** Val283 ***π-π*:** His263	1.20	92.30

The molecular docking study was performed according to previous work (Abbasi et al., 2022). A

molecular docking study was conducted to address the possible interactions between compound **6** and the enzyme's active site. The validation of docking was performed by re-docking the native ligand (tropolone) with the RMSD value lower than 2 Å as shown in Table 2 (Fitriana & Royani, 2022; Gaspersz & Sohilait, 2019; Mulyati & Panjaitan, 2021). The result of binding energy and the possible interactions is shown in Table 3. The result showed that compound **6** exhibited lower binding energy (-7.3 kcal/mol) compared with kojic acid as a positive control (-6.9 kcal/mol) and tropolone as a native ligand (-5.6 kcal/mol). This demonstrates a correlation between the inhibition value of compound **6** and kojic acid, where **6** showed almost the same interaction with the critical residue in the active site cavity of the enzyme, like a tropolone, as depicted in Tables 2 and 3. Nevertheless, **2** showed higher binding energy (-6.1 kcal/mol) than kojic acid and **6** and no interaction with copper ion in the active site due to steric hindrance, so **2** exhibited deficient inhibitory activity, as shown in Table 1. Therefore, **6** exhibited better inhibitory activity than kojic acid, as shown in Table 1.

Table 3. Docking binding energy and interactions over the tyrosinase with kojic acid, **2** and **6**.

Compound	Binding energy (kcal/mol)	Interactions over the tyrosinase
Kojic Acid (Positive Control)	-6.9	**van der Waals:** His61, His85, Phe90, His94, His259, Asn260, His263, Phe264, Met280, Gly281, Ser282, Val283, Ala286, Phe292, His296, Cu401 **Metal-Donor:** Cu400
2	-6.1	**Van der Walls**: Met257, Val248, Phe264, His61, Ala286, Met280, Ser282, Hys263, Gly281, Asn260, His259, His85, His244, Val283 **H-bond**: Asn260
6	-7.3	**van der Waals :** His61, Glu256, His259, Asn260, Phe264, Met280, Gly281, Ser282, Phe292, His296, Cu400 **Metal-Donor:** Cu401 ***π-σ*:** Val283 ***π-π*:** His263 ***π*-alkyl :** His85, His244, Ala286

CONCLUSION

Eight compounds (**1**-**8**) had been successfully synthesized using Friedel-Craft acylation catalyzed by zinc chloride as a Lewis acid in good to excellent yield. ^{1}H and ^{13}C NMR determined their structures. All compounds were evaluated for their inhibitory activity against the tyrosinase enzyme, and compound **6** exhibited a high inhibitory activity compared with kojic acid. This result was supported by a molecular docking study to address the binding interaction of the best potent compound. The *in vitro* and computational studies showed that compound **6** disclosed good critical interaction with the tyrosinase enzyme. Therefore, it demonstrates that compound **6** (4-heptanoly resorcinol) could be a potential compound for further study to obtain better therapeutic agents.

ACKNOWLEDGMENT

The Royal Golden Jubilee supported this work for Ph.D. program (No. PHD/0017/2561), Thailand Research Fund. The authors also would like to thank Prof. Dr. Yana M. Syah for his facility in computational chemistry.

REFERENCES

Abbasi, M. A., Siddiqui, S. Z., Nazir, M., Raza, H., Zafar, A., Shah, S. A., . . . Seo, S.-Y. (2022). Multi-Step Synthesis of Indole-N-Ethyltriazole Hybrids Amalgamated with N-Arylated Ethanamides: Structure-Activity Relationship and Mechanistic Explorations Through Tyrosinase Inhibition, Kinetics And Computational Ascriptions. *Journal of Molecular Structure*, *1261*, 132953.

Ashooriha, M., Khoshneviszadeh, M., Khoshneviszadeh, M., Moradi, S. E., Rafiei, A., Kardan, M., & Emami, S. (2019). 1,2,3-Triazole-Based Kojic Acid Analogs As Potent Tyrosinase

Inhibitors: Design, Synthesis And Biological Evaluation. *Bioorganic Chemistry, 82*, 414-422.

Berman, H., Henrick, K., & Nakamura, H. (2003). Announcing The Worldwide Protein Data Bank. *Nature Structural & Molecular Biology., 10*, 980-980.

Berman, H. M., Westbrook, J., Feng, Z., Gilliland, G., Bhat, T. N., Weissig, H., . . . Bourne, P. E. (2000). The Protein Data Bank. *Nucleic Acids Res., 28*, 235-242.

Bose, A., Petsko, G. A., & Eliezer, D. (2018). Parkinson's Disease and Melanoma: Co-Occurrence and Mechanisms. *Journal of Parkinson's Disease, 8*(3), 385-398.

Chen, W.-C., Tseng, T.-S., Hsiao, N.-W., Lin, Y.-L., Wen, Z.-H., Tsai, C.-C., . . . Tsai, K.-C. (2015). Discovery of Highly Potent Tyrosinase Inhibitor, T1, With Significant Anti-Melanogenesis Ability by Zebrafish in Vivo Assay and Computational Molecular Modeling. *Scientific Reports, 5(*7995), 1-8.

Choi, Y. K., Rho, Y. K., Yoo, K. H., Lim, Y. Y., Li, K., Kim, B. J., . . . Kim, D. S. (2010). Effects of Vitamin C Vs. Multivitamin on Melanogenesis: Comparative Study in Vitro and In Vivo. *International Journal of Dermatology., 49*, 218-226.

Chortani, S., Nimbarte, V. D., Horchani, M., Jannet, H. B., & Romdhane, A. (2019). Synthesis, Biological Evaluation and Molecular Docking Analysis of Novel Benzopyrimidinone Derivatives as Potential Anti-Tyrosinase Agents. *Bioorganic Chemistry, 92*, 103270.

Deri, B., Kanteev, M., Goldfeder, M., Lecina, D., Guallar, V., Adir, N., & Fishman, A. (2016). The Unravelling of The Complex Pattern of Tyrosinase Inhibition. *Scientific Reports, 6*, 34993.

Faig, J. J., Moretti, A., Joseph, L. B., Zhang, Y., Nova, M. J., Smith, K., & Uhrich, K. E. (2017). Biodegradable Kojic Acid-Based Polymers: Controlled Delivery of Bioactives for Melanogenesis Inhibition. *Biomacromolecules, 18*, 363-373.

Fitriana, A. S., & Royani, S. (2022). Molecular Docking Study of Chalcone Derivatives as Potential Inhibitors of SARS-CoV-2 Main Protease. *Indonesian Journal of Chemical Research, 9*(3), 150-162.

Gaspersz, N., & Sohilait, M. R. (2019). Penambatan Molekuler α, β, dan γ-mangostin Sebagai Inhibitor α-amilase Pankreas Manusia. *Indonesian Journal of Chemical Research, 6*(2), 59-66.

Hassan, M., Ashraf, Z., Abbas, Q., Raza, H., & Seo, S.-Y. (2018). Exploration of Novel Human Tyrosinase Inhibitors by Molecular Modeling, Docking and Simulation Studies. *Interdisciplinary Sciences: Computational Life Sciences, 10*, 68-80.

Ismaya, W. T., Rozeboom, H. J., Weijn, A., Mes, J. J., Fusetti, F., Wichers, H. J., & Dijkstra, B. W. (2011). Crystal structure of Agaricus Bisporus Mushroom Tyrosinase: Identity of The Tetramer Subunits and Interaction with Tropolone. *Biochemistry, 50*, 5477-5486.

Karakaya, G., Türe, A., Ercan, A., Öncül, S., & Aytemir, M. D. (2019). Synthesis, Computational Molecular Docking Analysis and Effectiveness on Tyrosinase Inhibition of Kojic Acid Derivatives. *Bioorganic Chemistry, 88*, 102950.

Larik, F. A., Saeed, A., Channar, P. A., Muqadar, U., Abbas, Q., Hassan, M., . . . Bolte, M. (2017). Design, Synthesis, Kinetic Mechanism and Molecular Docking Studies of Novel 1-Pentanoyl-3-Arylthioureas as Inhibitors of Mushroom Tyrosinase and Free Radical Scavengers. *European Journal of Medicinal Chemistry, 141*, 273-281.

Lee, S. Y., Baek, N., & Nam, T.-g. (2016). Natural, Semisynthetic and Synthetic Tyrosinase Inhibitors. *Journal of Enzyme Inhibition and Medicinal Chemistry, 31*, 1-13.

Liu, P., Xu, X., Chen, L., Ma, L., Shen, X., & Hu, L. (2014). Discovery and SAR Study of Hydroxyacetophenone Derivatives as Potent, Non-Steroidal Farnesoid X Receptor (FXR) Antagonists. *Bioorganic & Medicinal Chemistry, 22*, 1596-1607.

Mahdavi, M., Ashtari, A., Khoshneviszadeh, M., Ranjbar, S., Dehghani, A., Akbarzadeh, T., . . . Saeedi, M. (2018). Synthesis of New Benzimidazole-1, 2, 3-Triazole Hybrids as Tyrosinase Inhibitors. *Chemistry & Biodiversity, 15*, e1800120.

Mann, T., Gerwat, W., Batzer, J., Eggers, K., Scherner, C., Wenck, H., . . . Kolbe, L. (2018). Inhibition of Human Tyrosinase Requires Molecular Motifs Distinctively Different from Mushroom Tyrosinase. *Journal of Investigative Dermatology, 138*, 1601-1608.

Mulyati, B., & Panjaitan, R. S. (2021). Study of Molecular Docking of Alkaloid Derivative Compounds from Stem Karamunting

(Rhodomyrtus tomentosa) Against α-Glucosidase Enzymes. *Indo. J. Chem. Res.*, *9*, 129-136.

Noh, J.-M., Kwak, S.-Y., Seo, H.-S., Seo, J.-H., Kim, B.-G., & Lee, Y.-S. (2009). Kojic Acid-Amino Acid Conjugates as Tyrosinase Inhibitors. *Bioorganic & Medicinal Chemistry Letters*, *19*, 5586-5589.

Pillaiyar, T., Manickam, M., & Jung, S.-H. (2015). Inhibitors of Melanogenesis: A Patent Review (2009–2014). *Expert Opinion on Therapeutic Patents*, *25*, 775-788.

Pillaiyar, T., Manickam, M., & Namasivayam, V. (2017). Skin Whitening Agents: Medicinal Chemistry Perspective of Tyrosinase Inhibitors. *Journal of Enzyme Inhibition and Medicinal Chemistry*, *32*, 403-425.

Qiu, L., Chen, Q.-X., Wang, Q., Huang, H., & Song, K.-K. (2005). Irreversibly Inhibitory Kinetics of 3, 5-Dihydroxyphenyl Decanoate on Mushroom (Agaricus Bisporus) Tyrosinase. *Bioorganic & Medicinal Chemistry*, *13*, 6206-6211.

Silavi, R., Divsalar, A., & Saboury, A. A. (2012). A Short Review on The Structure–Function Relationship of Artificial Catecholase/Tyrosinase and nuclease activities of Cu-complexes. *Journal of Biomolecular Structure and Dynamics*, *30*, 752-772.